1

Fictitious Domain Methods for Incompressible Viscous Flow around Moving Rigid Bodies

R. Glowinski[1], T. W. Pan[1], J. Periaux[2]

[1]Department of Mathematics, University of Houston, Houston, Texas 77204, U. S. A.

[2]Dassault Aviation, 92214 Saint-Cloud, France

Abstract

In this article we discuss the application of a Lagrange multiplier based fictitious domain method to the numerical simulation of incompressible viscous flow modelled by the Navier-Stokes equations around moving bodies. The solution method combines finite element approximations, time discretization by operator splitting and conjugate gradient algorithms for the solution of the linearly constrained quadratic minimization problems coming from the splitting method. The results of several numerical experiments for two-dimensional flow around a moving disk are presented.

1.1 INTRODUCTION: PRINCIPLE, HISTORICAL FACTS AND SYNOPSIS

Supposed that $\Omega \subset \boldsymbol{R}^d$ (d=1, 2, 3) is a connected open set (a domain) containing an inclusion ω, as shown in Figure 1, below; we denote by Γ and γ the boundaries of Ω and ω, respectively. We consider now the following *boundary value problem*

$$A(u) = f \ \ in \ \ \Omega \setminus \overline{\omega}, \tag{1}$$

$$B_0(u) = g_0 \ \ on \ \ \Gamma, \tag{2}$$

$$B_1(u) = g_1 \ \ on \ \ \gamma, \tag{3}$$

where, in (1)-(3), the functions f, g_0, g_1, and operators A, B_0, B_1, are given.

[0] This paper will appear in the proceedings of MAFELAP 1996, Brunel University, June 25-28, 1996, UK.

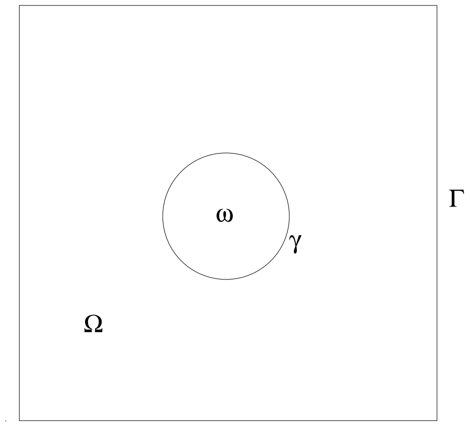

Figure 1 Geometry of Problem (1)-(3)

Assuming that the shape of Ω is *simple* (which is clearly the case for the example of Figure 1) it is reasonable to want to take advantage of that simplicity when solving problem (1)-(3) numerically; indeed, it may allow, among other things, the use of *regular finite difference or finite element meshes* and consequently of *fast solvers* for the finite dimensional systems approximating problem (1)-(3) on these grids. In order to address this goal a reasonable idea is to replace problem (1)-(3) by the following problem:

Find $\tilde{u}$ defined over Ω, S_γ a measure supported by γ, so that

$$\tilde{A}(\tilde{u}) = \tilde{f} + S_\gamma \text{ in } \Omega, \tag{4}$$

$$\tilde{B}_0(\tilde{u}) = g_0 \text{ on } \Gamma, \tag{5}$$

$$\tilde{B}_1(\tilde{u}|_{\Omega\setminus\overline{\omega}}) = g_1 \text{ on } \gamma; \tag{6}$$

in (4)-(6), operator $\tilde{A}$ is an operator of the same type than A, which concides - in some sense - with A on $\Omega \setminus \overline{\omega}$, $\tilde{f}$ is some extension of f over Ω and $\tilde{B}_0$, $\tilde{B}_1$ are extensions of B_0, B_1.

If S_γ is *well-chosen*, so that the corresponding solution of the boundary value problem (4), (5) satisfies relation (6) we can expect to have $\tilde{u}|_{\Omega\setminus\overline{\omega}} = u$, where u is the solution of problem (1)-(3). At that stage, several comments are in order:

Remark 1. There are other ways to "embed" domain $\Omega \setminus \overline{\omega}$, in the larger domain Ω. We can use *penalty*, for example, as shown in ref. [1].

Remark 2. Fictitious domain methods can also be applied to time dependent problems as shown in this article (see also [2]-[6]).

Remark 3. There is no particular difficulty to replace ω by a finite number of "holes", ω_1, ω_2, ..., ω_q, with $q \geq 2$.

Remark 4. Most references on fictitious domain methods are concerned by application to *linear problems.* Actually, these methods are also well-suited to the solution of *nonlinear problems* as shown, for example, in [3]-[6] (and in the present article). □

To our knowledge fictitious domain techniques for the solution of partial differential equations have been advocated for the first time, more than thirty years ago, by various investigators of the Marchuk-Yanenko school of Numerical Mathematics, at Novossibirsk. These methods belong, essentially, to the class of *boundary fitted* fictitious domain methods, since the discretization is taking place on a mesh which is a regular one with the exception of a neighborhood of γ where the mesh is locally distorted in order to fit accurately the boundary γ. This approach has motivated a *very* large number of publications; we shall limit our references to [7]-[9] which are typical examples of the Novossibirsk fictitious domain methodology (see also the references therein). In the early seventies G.H. Golub and collaborators introduced a *domain embedding* technique for elliptic problems where, once again, the mesh has to follow the boundary γ (see ref. [10] for details). The fictitious domain methods discussed in the present article are closer to the method advocated by Ch. Peskin in [11]; indeed, in [11] Peskin uses a fictitious domain method to simulate blood flow around heart valves (natural or artificial), the flow being modelled by the incompressible Navier-Stokes equations. An important analogy between the work in [11] and the present article is that in both cases one uses a mesh which is nonfitted to γ, and which therefore *can stay fixed even if* γ *moves.* More recently, R. Leveque and collaborators have developed in [12] a method closely related to Peskin's one.

In this article, motivated by the simulation of *Navier-Stokes flow around moving rigid bodies*, we shall follow Peskin philosophy in the sense that we shall not use body fitted meshes; also - unlike Peskin - we shall make a systematic use of *variational principles* and of a *Lagrange multiplier* to enforce the boundary condition on γ. In fact the Lagrange multiplier will be the measure S_γ in equation (4). The content of this article is as follows:

In Section 2 we shall formulate a model flow problem governed by the incompressible Navier-Stokes equations. A Lagrange multiplier/fictitious domain based variational formulation of the above problem will be given in Section 3. In Section 4, we shall describe a finite element approximation of the above variational problem, while in Section 5 we shall discuss its time discretization by operator splitting methods à la Marchuk-Yanenko. In Section 6 we shall discuss the solution of the various sub-problems associated to the splitting method, and finally, in Section 7, we shall present the results of numerical experiments.

Remark 5. The present article is not a close repetition of the Navier-Stokes/fictitious domain methods related parts of refs. [4]-[6]. Indeed in the above articles the incompressibility condition was forced via a *Stokes solver* à la Cahouet-Chabard (see refs. [13]-[18]), while in this chapter we shall use a L^2-*projection method*, closely related to the one used in, e.g., [19] (see also the references therein).

1.2 FORMULATION OF A MODEL PROBLEM

The geometrical situation being like in Figure 1 (with d =2, 3) with $\omega = \omega(t)$ a *moving rigid body* we consider for $t \geq 0$ the solution of the following system of Navier-Stokes equations

$$\frac{\partial \mathbf{u}}{\partial t} - \nu \Delta \mathbf{u} + (\mathbf{u} \cdot \nabla)\mathbf{u} + \nabla p = \mathbf{f} \; in \; \Omega \setminus \overline{\omega(t)}, \tag{7}$$

$$\nabla \cdot \mathbf{u} = 0 \; in \; \Omega \setminus \overline{\omega(t)}, \tag{8}$$

$$\mathbf{u}(\mathbf{x}, 0) = \mathbf{u}_0(\mathbf{x}), \quad \mathbf{x} \in \Omega \setminus \overline{\omega(0)}, (with \; \nabla \cdot \mathbf{u}_0 = 0), \tag{9}$$

$$\mathbf{u} = \mathbf{g}_0 \; on \; \Gamma, \tag{10}$$

$$\mathbf{u} = \mathbf{g}_1 \; on \; \gamma(t). \tag{11}$$

In (7)-(11), $\mathbf{u}$ and p denote as usual *velocity* and *pressure*, respectively; $\nu(> 0)$ is a *viscosity* coefficient, $\mathbf{f}$ a density of *external forces*, $\mathbf{x}$ the *generic point* of $\boldsymbol{R}^d$ ($\mathbf{x} = \{x_i\}_{i=1}^d$), $\gamma(t) = \partial\omega(t)$ and

$$(\mathbf{u} \cdot \nabla)\mathbf{u} = \{\sum_{j=1}^{j=d} u_j \frac{\partial u_i}{\partial x_j}\}_{i=1}^{i=d}.$$

We suppose that

$$\int_\Gamma \mathbf{g}_0 \cdot \mathbf{n} \, d\Gamma = 0, \quad \int_{\gamma(t)} \mathbf{g}_1 \cdot \mathbf{n} \, d\gamma = 0, \tag{12}$$

where, in (12), $\mathbf{n}$ is the outer normal unit vector at $\partial(\Omega \setminus \overline{\omega(t)})$; if $\mathbf{g}_1$ is the velocity associated to a rigid body motion the second condition in (12) is automatically satisfied. In the following, we shall use, if necessary, the notation $\phi(t)$ for the function

$$\mathbf{x} \to \phi(\mathbf{x}, t).$$

The existence of solution for problem (7)-(11) is a nontrial mathematical issue *when ω is moving*; we shall not address it in this article (see however [20] and the references therein).

1.3 A LAGRANGE MULTIPLIER/FICTITIOUS DOMAIN VARIATIONAL FORMULATION OF PROBLEM (7)-(11)

We introduce first the following functional spaces

$$\mathbf{V}_{\mathbf{g}_0(t)} = \{\mathbf{v} | \mathbf{v} \in (\mathbf{H}^1(\Omega))^d, \mathbf{v} = \mathbf{g}_0(t) \; on \; \Gamma\}, \tag{13}$$

$$\mathbf{V}_0 = (\mathbf{H}_0^1(\Omega))^d, \tag{14}$$

$$L_0^2(\Omega) = \{q | q \in L^2(\Omega); \int_\Omega q \, d\mathbf{x} = 0\}, \tag{15}$$

$$\Lambda(t) = (\mathbf{H}^{-1/2}(\gamma(t)))^d. \tag{16}$$

We consider next $\mathbf{U}_0$ (resp., $\tilde{\mathbf{f}}$) such that

$$\nabla \cdot \mathbf{U}_0 = 0, \;\; \mathbf{U}_0|_{\Omega\setminus\overline{\omega(0)}} = \mathbf{u}_0, \tag{17}$$

(resp., $\tilde{\mathbf{f}}|_{\Omega\setminus\overline{\omega}} = \mathbf{f}$).

It can be shown - at least formally - that problem (7)-(11) is *equivalent* to:

For $t \geq 0$, *find* $\{\mathbf{U}(t), P(t), \lambda(t)\} \in \mathbf{V}_{\mathbf{g}_0(t)} \times L^2_0(\Omega) \times \Lambda(t)$ *such that*

$$\int\limits_\Omega \frac{\partial \mathbf{U}}{\partial t} \cdot \mathbf{v}\, d\mathbf{x} + \nu \int\limits_\Omega \nabla \mathbf{U} \cdot \nabla \mathbf{v}\, d\mathbf{x} + \int\limits_\Omega (\mathbf{U} \cdot \nabla)\mathbf{U} \cdot \mathbf{v}\, d\mathbf{x} - \int\limits_\Omega P \nabla \cdot \mathbf{v}\, d\mathbf{x}$$

$$= \int\limits_\Omega \tilde{\mathbf{f}} \cdot \mathbf{v}\, d\mathbf{x} + \int\limits_{\gamma(t)} \lambda \cdot \mathbf{v}\, d\gamma, \; \forall \mathbf{v} \in \mathbf{V}_0, \tag{18}$$

$$\nabla \cdot \mathbf{U}(t) = 0, \tag{19}$$

$$\mathbf{U}(0) = \mathbf{U}_0, \tag{20}$$

$$\mathbf{U}(t) = \mathbf{g}_1(t) \; \mathit{on} \; \gamma(t), \tag{21}$$

in the sense that

$$\mathbf{U}(t)|_{\Omega\setminus\overline{\omega}} = \mathbf{u}, \;\; P|_{\Omega\setminus\overline{\omega}} = p; \tag{22}$$

it is very easily shown that

$$\lambda = [\nu \frac{\partial \mathbf{U}}{\partial \mathbf{n}} - \mathbf{n}P]_\gamma. \tag{23}$$

where $[\quad]_\gamma$ denotes the jump at γ.

Remark 6. For $\tilde{\mathbf{f}}$ we can take an L^2-extension of $\mathbf{f}$ (by $\mathbf{0}$ for example).

Remark 7. We observe that the actual geometry, i.e. $\omega(t)$ and $\gamma(t)$, occurs "only" through the $\gamma(t)$-integral in (18) and in (21).

1.4 FINITE ELEMENT APPROXIMATION OF PROBLEM (18)-(21)

We suppose that $\Omega \subset \boldsymbol{R}^2$ ($d = 2$). With h a *space discretization step* we introduce a finite element triangulation $\mathcal{T}_h$ of $\overline{\Omega}$ and then $\mathcal{T}_{2h}$ a triangulation twice coarser (in practice we should construct $\mathcal{T}_{2h}$ first and then $\mathcal{T}_h$ by joining the midpoints of the edges of $\mathcal{T}_{2h}$, dividing thus each triangle of $\mathcal{T}_{2h}$ into 4 similar subtriangles). We define then the following finite dimensional spaces which approximate $\mathbf{V}_{\mathbf{g}_0(t)}$, $\mathbf{V}_0$, $L^2(\Omega)$, $L^2_0(\Omega)$, respectively:

$$\mathbf{V}_{\mathbf{g}_{0h}} = \{\mathbf{v}_h | \mathbf{v}_h \in C^0(\bar{\Omega})^2, \; \mathbf{v}_h|_T \in P_1 \times P_1, \; \forall T \in \mathcal{T}_h, \; \mathbf{v}_h|_\Gamma = \mathbf{g}_{0h}\}, \tag{24}$$

$$\mathbf{V}_{0h} = \{\mathbf{v}_h | \mathbf{v}_h \in C^0(\bar{\Omega})^2, \; \mathbf{v}_h|_T \in P_1 \times P_1, \; \forall T \in \mathcal{T}_h, \; \mathbf{v}_h|_\Gamma = \mathbf{0}\}, \tag{25}$$

$$L^2_h = \{q_h | q_h \in C^0(\bar{\Omega}), \; q_h|_T \in P_1, \; \forall T \in \mathcal{T}_{2h}\}, \tag{26}$$

$$L^2_{0h} = \{q_h | q_h \in L^2_h, \; \int\limits_\Omega q_h\, d\mathbf{x} = 0\}; \tag{27}$$

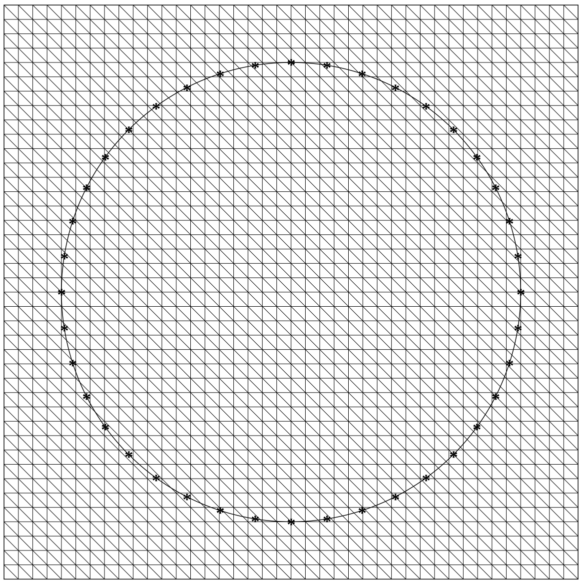

Figure 2 Part of the triangulation of Ω with mesh points indicated by "$*$" on the disk boundary

in (24), $\mathbf{g}_{0h}$ is an approximation of $\mathbf{g}_0$ satisfying $\int_\Gamma \mathbf{g}_{0h} \cdot \mathbf{n}\, d\Gamma = 0$.
Concerning the space $\Lambda_h(t)$ approximating $\Lambda(t)$, we define it by

$$\Lambda_h(t) = \{\mu_h | \mu_h \in (L^\infty(\gamma(t)))^2, \mu_h \, \textit{is constant on the arc joining} \\ 2 \, \textit{consecutive mesh points on} \, \gamma(t)\}. \tag{28}$$

A particular choice for the mesh points on γ is visualized on Figure 2 where ω is a disk.

Let us mention that the mesh points on γ *do not have to be* at the intersection of γ with the triangle edges; as shown in [21] one still has convergence properties (for elliptic problems at least) if $h_\gamma \geq C h_\Omega$ with C of the order of 3 (numerical experiments suggest that $C = 2\sqrt{2}$). This kind of decoupling between the Ω and γ meshes makes the fictitious domain approach very attractive for problems with moving boundaries, like those addressed in this article.

With the above spaces it is quite natural to approximate problem (18)-(21) (with obvious notation) by:

$$\int_\Omega \frac{\partial \mathbf{U}_h}{\partial t} \cdot \mathbf{v}\, d\mathbf{x} + \nu \int_\Omega \nabla \mathbf{U}_h \cdot \nabla \mathbf{v}\, d\mathbf{x} + \int_\Omega (\mathbf{U}_h \cdot \nabla)\mathbf{U}_h \cdot \mathbf{v}\, d\mathbf{x} - \int_\Omega P_h \nabla \cdot \mathbf{v}\, d\mathbf{x} \\ = \int_\Omega \tilde{\mathbf{f}}_h \cdot \mathbf{v}\, d\mathbf{x} + \int_{\gamma(t)} \lambda_h \cdot \mathbf{v}\, d\gamma, \; \forall \mathbf{v} \in \mathbf{V}_{0h}, \tag{29}$$

$$\int_\Omega q\nabla \cdot \mathbf{U}_h(t)\, d\mathbf{x} = 0,\ \forall q \in L_h^2, \tag{30}$$

$$\mathbf{U}_h(0) = \mathbf{U}_{0h}, \tag{31}$$

$$\int_{\gamma(t)} (\mathbf{U}_h(t) - \mathbf{g}_1(t)) \cdot \mu\, d\gamma = 0,\ \forall \mu \in \Lambda_h(t), \tag{32}$$

$$\{\mathbf{U}_h(t), P_h(t), \lambda_h(t)\} \in \mathbf{V}_{\mathbf{g}_0(t)h} \times L_{0h}^2 \times \Lambda_h(t); \tag{33}$$

in (31), $\mathbf{U}_{0h}$ is an approximation of $\mathbf{U}_0$ so that

$$\int_\Omega q\nabla \cdot \mathbf{U}_{0h}\, d\mathbf{x} = 0,\ \forall q \in L_h^2.$$

The time discretization of problem (29)-(33) by operator splitting methods will be discussed in Section 5.

1.5 TIME DISCRETIZATION OF PROBLEM (29)-(33) BY OPERATOR SPLITTING METHODS

Most "modern" Navier-Stokes solvers are based on operator splitting algorithms in order to force the incompressibility condition via a Stokes solver or a L^2- projection method (see refs. [18], [19] for details). This approach still applies to the initial value problem (29)-(33). Indeed this problem contains three numerical difficulties to each of which can be associated a specific operator, namely

1. The incompressibility condition and the related unknown pressure.
2. An advection-diffusion term.
3. The boundary condition on $\gamma(t)$ and the related multiplier $\lambda(t)$.

The operators in (1) and (3) are essentially *projection operators.*

From an abstract point of view problem (29)-(33) is a particular case of the following class of initial value problems

$$\begin{cases} \dfrac{d\phi}{dt} + A_1(\phi) + A_2(\phi) + A_3(\phi) = f, \\ \phi(0) = \phi_0, \end{cases} \tag{34}$$

where operators A_i can be *multivalued.* Among the many operator splitting schemes which can be employed to solve (34) we shall advocate the very simple one below (analyzed in, e.g., [22]); it is only first order accurate, but its low order accuracy is compensated by good stability and robustness properties.

A fractional step scheme à la Marchuk-Yanenko:

In the following, $\triangle t$ is a time discretization step.

$$\phi^0 = \phi_0, \tag{35}$$

for $n \geq 0$, *we obtain* ϕ^{n+1} *from* ϕ^n *via the solution of*

$$\frac{\phi^{n+1/3}-\phi^n}{\triangle t}+A_1(\phi^{n+1/3})=f_1^{n+1}, \tag{36}$$

$$\frac{\phi^{n+2/3}-\phi^{n+1/3}}{\triangle t}+A_2(\phi^{n+2/3})=f_2^{n+1}, \tag{37}$$

$$\frac{\phi^{n+1}-\phi^{n+2/3}}{\triangle t}+A_3(\phi^{n+1})=f_3^{n+1}, \tag{38}$$

with $\sum_{i=1}^{3} f_i^{n+1}=f^{n+1}$.

Applying the above scheme to problem (29)-(33) we obtain (with $0 \leq \alpha, \beta \leq 1$, $\alpha+\beta=1$ and after dropping some of the subscripts h):

$$\mathbf{U}^0=\mathbf{U}_{0h}; \tag{39}$$

for $n \geq 0$, *we compute* $\{\mathbf{U}^{n+1/3}, P^{n+1/3}\}$, $\mathbf{U}^{n+2/3}$, $\{\mathbf{U}^{n+1}, \lambda^{n+1}\}$ *via the solution of*

$$\begin{cases} \displaystyle\int_\Omega \frac{\mathbf{U}^{n+1/3}-\mathbf{U}^n}{\triangle t}\cdot\mathbf{v}\,d\mathbf{x}-\int_\Omega P^{n+1/3}\nabla\cdot\mathbf{v}\,d\mathbf{x}=0,\ \forall\mathbf{v}\in\mathbf{V}_{0h}, \\ \displaystyle\int_\Omega q\nabla\cdot\mathbf{U}^{n+1/3}\,d\mathbf{x}=0,\ \forall q\in L_h^2;\ \mathbf{U}^{n+1/3}\in\mathbf{V}_{\mathbf{g}_{0h}}^{n+1},\ P^{n+1/3}\in L_{0h}^2, \end{cases} \tag{40}$$

$$\begin{cases} \displaystyle\int_\Omega \frac{\mathbf{U}^{n+2/3}-\mathbf{U}^{n+1/3}}{\triangle t}\cdot\mathbf{v}\,d\mathbf{x}+\alpha\nu\int_\Omega\nabla\mathbf{U}^{n+2/3}\cdot\nabla\mathbf{v}\,d\mathbf{x} \\ \displaystyle\quad+\int_\Omega(\mathbf{U}^{n+1/3}\cdot\nabla)\mathbf{U}^{n+2/3}\cdot\mathbf{v}\,d\mathbf{x}=\alpha\int_\Omega\tilde{\mathbf{f}}^{n+1}\cdot\mathbf{v}\,d\mathbf{x},\ \forall\mathbf{v}\in\mathbf{V}_{0h}; \\ \mathbf{U}^{n+2/3}\in\mathbf{V}_{\mathbf{g}_{0h}}^{n+1}, \end{cases} \tag{41}$$

$$\begin{cases} \displaystyle\int_\Omega \frac{\mathbf{U}^{n+1}-\mathbf{U}^{n+2/3}}{\triangle t}\cdot\mathbf{v}\,d\mathbf{x}+\beta\nu\int_\Omega\nabla\mathbf{U}^{n+1}\cdot\nabla\mathbf{v}\,d\mathbf{x} \\ \displaystyle\quad=\beta\int_\Omega\tilde{\mathbf{f}}^{n+1}\cdot\mathbf{v}\,d\mathbf{x}+\int_{\gamma^{n+1}}\lambda^{n+1}\cdot\mathbf{v}\,d\gamma,\ \forall\mathbf{v}\in\mathbf{V}_{0h}, \\ \displaystyle\int_{\gamma^{n+1}}(\mathbf{U}^{n+1}-\mathbf{g}_{1h}^{n+1})\cdot\mu\,d\gamma=0,\ \forall\mu\in\Lambda_h^{n+1}; \\ \mathbf{U}^{n+1}\in\mathbf{V}_{\mathbf{g}_{0h}}^{n+1},\lambda^{n+1}\in\Lambda_h^{n+1}. \end{cases} \tag{42}$$

In (40)-(42) we have used the following notation

$$\mathbf{V}_{\mathbf{g}_{0h}}^{n+1}=\mathbf{V}_{\mathbf{g}_0((n+1)\triangle t)h},\ \ \Lambda_h^{n+1}=\Lambda_h((n+1)\triangle t).$$

Remark 8. Many other splitting schemes are possible, some more complicated (and accurate) than the one above; on the other hand, scheme (35)-(38) is the simplest splitting scheme for those situations involving three operators and the results obtained with it compare favorablely with those obtained by more sophisticated schemes (for the particular problem considered here, at least).

1.6 SOLUTION OF THE SUBRPOBLEMS (40), (41) AND (42)

1.6.1 SOLUTION OF THE SUBPROBLEM (40): L^2-PROJECTION ON $\mathbf{V}_{\mathbf{g}_{0h}}$

The subproblems (40) can be viewed as *degenerated (zero viscosity) quasi-Stokes problems* of the following form (some h and n have been dropped):

$$\alpha \int_\Omega \mathbf{U} \cdot \mathbf{v}\, d\mathbf{x} - \int_\Omega P \nabla \cdot \mathbf{v}\, d\mathbf{x} = \int_\Omega \mathbf{f} \cdot \mathbf{v}\, d\mathbf{x},\ \forall \mathbf{v} \in \mathbf{V}_{0h}, \tag{43}$$

$$\int_\Omega q \nabla \cdot \mathbf{U}\, d\mathbf{x} = 0,\ \forall q \in L_h^2, \tag{44}$$

with $\{\mathbf{U}, P\} \in \mathbf{V}_{\mathbf{g}_{0h}} \times L_{0h}^2$ (and $\alpha = 1/\triangle t$).

It is very easy to interpret $\mathbf{U}$ in (43), (44); it is the L^2-projection of $\mathbf{f}/\alpha$ on the subspace of $\mathbf{V}_{\mathbf{g}_{0h}}$ consisting of those functions satisfying

$$\int_\Omega q \nabla \cdot \mathbf{v}\, d\mathbf{x} = 0,\ \forall q \in L_h^2. \tag{45}$$

The pressure P is the Lagrange multiplier associated to the linear constrains (45); P is *nonunique* unless we specify an additional relation, like - for example - $\int_\Omega P\, d\mathbf{x} = 0$, i.e. $P \in L_{0h}^2$.

The *saddle-point problem* (43), (44) can be solved by an *Uzawa/ Preconditioned Conjugate Gradient algorithm* operating in the space L_{0h}^2. This algorithm is as follows:

Step 0: Initialization

$$P^0 \in L_{0h}^2 \text{ is given;} \tag{46}$$

solve the projection problem:

$$\begin{cases} \alpha \int_\Omega \mathbf{U}^0 \cdot \mathbf{v}\, d\mathbf{x} = \int_\Omega \mathbf{f} \cdot \mathbf{v}\, d\mathbf{x} + \int_\Omega P^0 \nabla \cdot \mathbf{v}\, d\mathbf{x}\ \forall \mathbf{v} \in \mathbf{V}_{0h}; \\ \mathbf{U}^0 \in \mathbf{V}_{\mathbf{g}_{0h}}, \end{cases} \tag{47}$$

then

$$\begin{cases} \int_\Omega r^0 q\, d\mathbf{x} = \int_\Omega q \nabla \cdot \mathbf{U}^0\, d\mathbf{x},\ \forall q \in L_{0h}^2, \\ r^0 \in L_{0h}^2, \end{cases} \tag{48}$$

and finally

$$\begin{cases} \int_\Omega \nabla g^0 \cdot \nabla q \, d\mathbf{x} = \int_\Omega r^0 q \, d\mathbf{x}, \ \forall q \in L_h^2, \\ g^0 \in L_{0h}^2. \end{cases} \tag{49}$$

Take

$$w^0 = g^0. \tag{50}$$

Then for $k \geq 0$, assuming that P^k, r^k, g^k, w^k are known, compute P^{k+1}, r^{k+1}, g^{k+1}, w^{k+1} as follows:

Step 1: Descent

Solve:

$$\begin{cases} \alpha \int_\Omega \overline{\mathbf{U}}^k \cdot \mathbf{v} \, d\mathbf{x} = \int_\Omega w^k \nabla \cdot \mathbf{v} \, d\mathbf{x}, \ \forall \mathbf{v} \in \mathbf{V}_{0h}; \\ \overline{\mathbf{U}}^k \in \mathbf{V}_{0h}, \end{cases} \tag{51}$$

then

$$\begin{cases} \int_\Omega \bar{r}^k q \, d\mathbf{x} = \int_\Omega q \nabla \cdot \overline{\mathbf{U}}^k \, d\mathbf{x}, \ \forall q \in L_{0h}^2, \\ \bar{r}^k \in L_{0h}^2, \end{cases} \tag{52}$$

and finally

$$\begin{cases} \int_\Omega \nabla \bar{g}^k \cdot \nabla q \, d\mathbf{x} = \int_\Omega \bar{r}^k q \, d\mathbf{x}, \ \forall q \in L_h^2, \\ \bar{g}^k \in L_{0h}^2. \end{cases} \tag{53}$$

Compute

$$\rho_k = \int_\Omega r^k g^k \, d\mathbf{x} \Big/ \int_\Omega \bar{r}^k w^k \, d\mathbf{x}, \tag{54}$$

and then

$$P^{k+1} = P^k - \rho_k w^k, \tag{55}$$

$$g^{k+1} = g^k - \rho_k \bar{g}^k, \tag{56}$$

$$r^{k+1} = r^k - \rho_k \bar{r}^k. \tag{57}$$

Step 2: Convergence Testing and Construction of the New Descent Direction

If

$$\int_{\Omega} r^{k+1} g^{k+1}\, d\mathbf{x} \Big/ \int_{\Omega} r^0 g^0\, d\mathbf{x} \leq \epsilon, \tag{58}$$

take $P = P^{k+1}$ *and compute* $\mathbf{U}$ *from relation (43). Else, compute*

$$\gamma_k = \int_{\Omega} r^{k+1} g^{k+1}\, d\mathbf{x} \Big/ \int_{\Omega} r^k g^k\, d\mathbf{x} \tag{59}$$

and set

$$w^{k+1} = g^{k+1} + \gamma_k w^k. \tag{60}$$

Do $k = k+1$ *and go back to* (51).
The choice of ϵ in the stopping test (58) will be discussed in Section 7.

Remark 9. Using the trapezoidal rule to evaluate the various $L^2(\Omega)$-integrals in (40)-(42) and in algorithm (46)-(60) makes very easy and ecomomical the implementation of the above algorithm.

1.6.2 SOLUTION OF THE SUBPROBLEMS (41)

The solution by least squares/preconditioned conjugate gradient methods of linear or nonlinear advection-diffusion problems such as (41) has been discussed at length in [14], [15], [18] (see also [23]). Due to page limitation we shall skip it in the present article. Let us mention that iterative methods like GMRES can also be used to solve problems such as (40).

1.6.3 SOLUTION OF THE SUBPROBLEMS (42): FORCING THE DIRICHLET CONDITIONS ON γ

If $\beta > 0$, problem (42) is indeed a *saddle-point problem* whose solution has been discussed in [3], [4]. It can be solved by an Uzawa/conjugate gradient algorithm operating in the space Λ_h^{n+1}. For *two-dimensional* problems an efficient preconditioning operator is provided by a discrete version of the boundary operator $(\frac{\triangle t}{\beta\nu} I - \frac{\partial^2}{\partial s^2})^{-1/2}$, where s is the arc-length along γ (see [3] for details and computational experiments).

In the particular case where $\beta = 0$, problem (42) reduces to an $L^2(\Omega)$-projection over the subspace of $\mathbf{V}_{\mathbf{g}_{0h}}^{n+1}$ of the functions satisfying the condition

$$\int_{\gamma^{n+1}} (\mathbf{v} - \mathbf{g}_{1h}^{n+1}) \cdot \mu\, d\gamma = 0,\ \forall \mu \in \Lambda_h^{n+1}.$$

It follows from the above observation that if $\beta = 0$, problem (42) can be solved by an Uzawa/conjugate gradient algorithm operating in the space Λ_h^{n+1}, which has many similarities with algorithm (46)-(60). If one uses the trapezoidal rule to compute the various $L^2(\Omega)$-integrals in (42), taking $\beta = 0$ brings further simplification since in that particular case $\mathbf{U}^{n+1}$ will coincide with $\mathbf{U}^{n+2/3}$ at those vertices of $\mathcal{T}_h$ such that the support of the related shape function does not intersect γ^{n+1}; from the above observation it follows that to obtain $\mathbf{U}^{n+1}$ and λ^{n+1} we have to solve a linear system of the following form

$$\begin{cases} A\mathbf{x} + B^t\mathbf{y} & = \mathbf{b}, \\ B\mathbf{x} & = \mathbf{c}, \end{cases} \tag{61}$$

where A is a $N \times N$ matrix, symmetric and positive definite and where B is a $N \times M$ matrix; we have M and N both of the order of $1/h$. The saddle-point problem (61) can be solved also by an Uzawa/conjugate gradient algorithm operating in $\boldsymbol{R}^M$ (other methods are possible).

1.7 NUMERICAL EXPERIMENTS

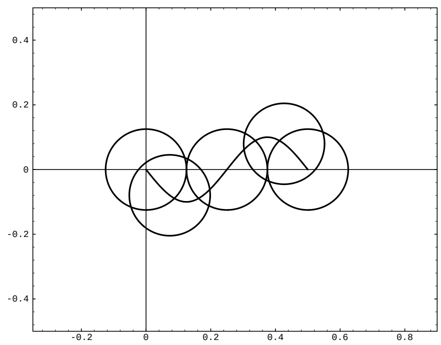

Figure 3

For the test problem that we consider, we shall simulate a two-dimensional flow with $\Omega = (-0.35, 0.9) \times (-0.5, 0.5)$ (see Figure 3) and ω a moving disk of radius 0.125. The center of the disk is moving between $(0,0)$ and $(0.5,0)$ along a prescribed trajectory $(x(t), y(t))$ (see Figure 3) given as follows

$$x(t) = 0.25(1 - \cos(\frac{\pi t}{2})), \qquad y(t) = -0.1\sin(\pi(1 - \cos(\frac{\pi t}{2})));$$

we have thus a *periodic* motion of period 4. Several different positions of the disk have been shown on Figure 3. The boundary conditions are $\mathbf{u} = \mathbf{0}$ on Γ and $\mathbf{u}$ on $\partial\omega(t)$ coinciding with the disk velocity.

We suppose that the disk rotates counterclockwisely at angular velocity π. Since we are taking $\nu = 10^{-2}$ the maximum Reynold's number based on the disk diameter as characteristic length is 25.584. On Ω we have used a regular triangulation $\mathcal{T}_h$ to approximate the velocity, like the one in Figure 2, the pressure grid $\mathcal{T}_{2h}$ being twice coarser. Concerning $\Lambda_h(t)$, $\gamma(t)$ has been divided into M subarcs of equal length.

We have run two series of tests: For the first series we have taken $h = 1/128$, $\triangle t = 0.0025$ and $M = 80$. For the second we have taken $h = 1/256$, $\triangle t = 0.00125$ and $M = 160$. With stopping criteria of the order of 10^{-12} we need around 10 iterations at most to have convergence of the conjugate gradient algorithms used to solve the problems at each step of scheme (39)-(42).

On Figures 4 and 5 (resp., 6 and 7) we show the isobar contours, the vorticity density and the streamlines obtained at $t = 4.5, 5, 5.5, 6, 6.5, 7, 7.5, 8$ for $h = 1/128$, $\triangle t = 0.0025$ and $M = 80$ (resp., $h = 1/256$, $\triangle t = 0.00125$ and $M = 160$). There is a good agreement between those results, concerning particularly streamlines and vorticity density. In order to improve pressure convergence we intend to consider more sophisticated methods with a stronger coupling between the steps of scheme (39)-(42). The corresponding results will be reported in a forthcoming publication.

1.8 ACKNOWLEDGEMENTS

We would like to acknowledge the helpful comments and suggestions of E. J. Dean, J.W. He, D.D. Joseph, Y. Kuznetsov, B. Maury, A.H. Sameh and F.J. Sanchez.

The support of the following institutions is acknowledged: University of Houston and Department of Computer Science, University of Minnesota. We also benefited from the support of NSF (Grants DMS 8822522, DMS 9112847, DMS 9217374), DRET (Grant 89424), DARPA (Contracts AFOSR F49620-89-C-0125 and AFOSR-90-0334), the Texas Board of Higher Education (Grants 003652156ARP and 003652146ATP), University of Houston (PEER grant 1-27682) and again NSF under the HPCC Grand Challenge Grant ECS-9527123.

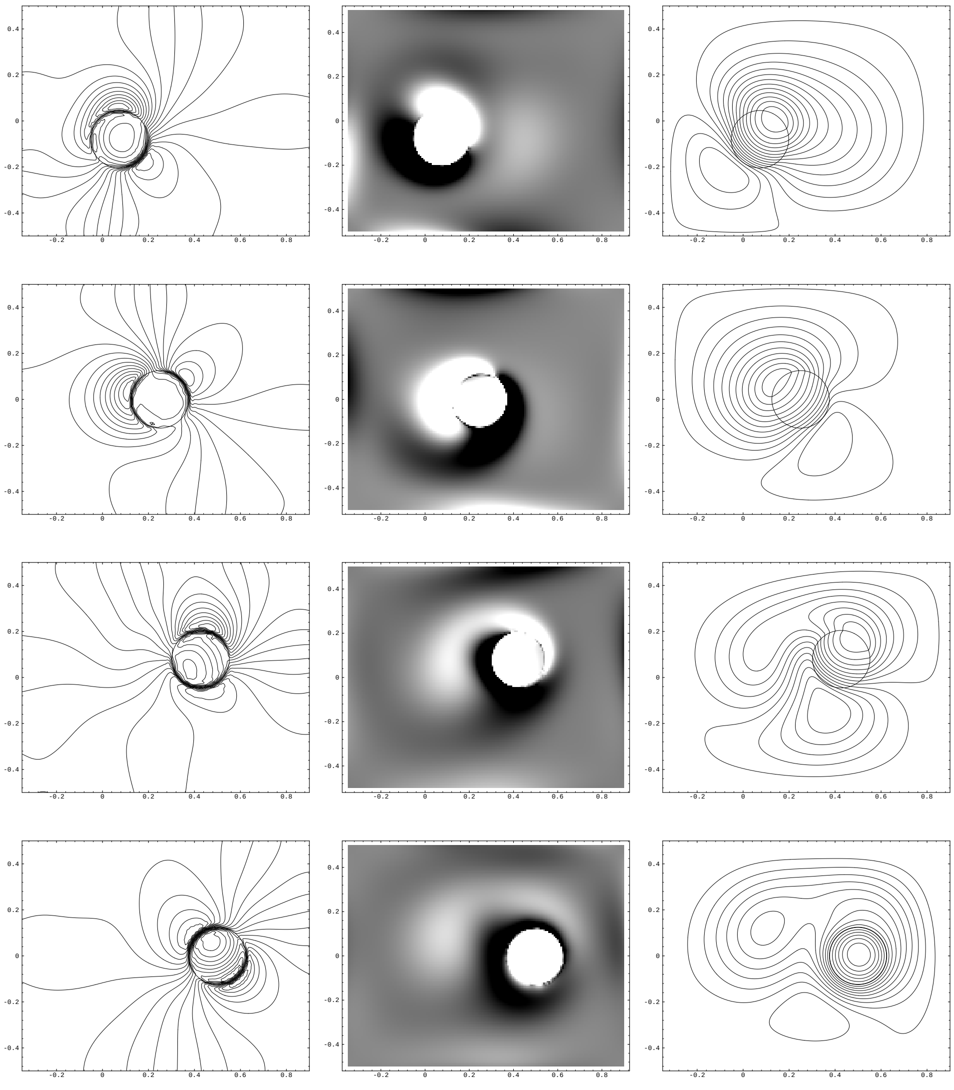

Figure 4 Isobar contours (at left), vorticity density (at middle) and streamlines (at right) at time $t = 4.5$, 5, 5.5, 6 during first half of one period of the disk motion. The disk is moving from the left to the right. The mesh size for velocity is $h = 1/128$ and the mesh size for pressure is $h = 1/64$.

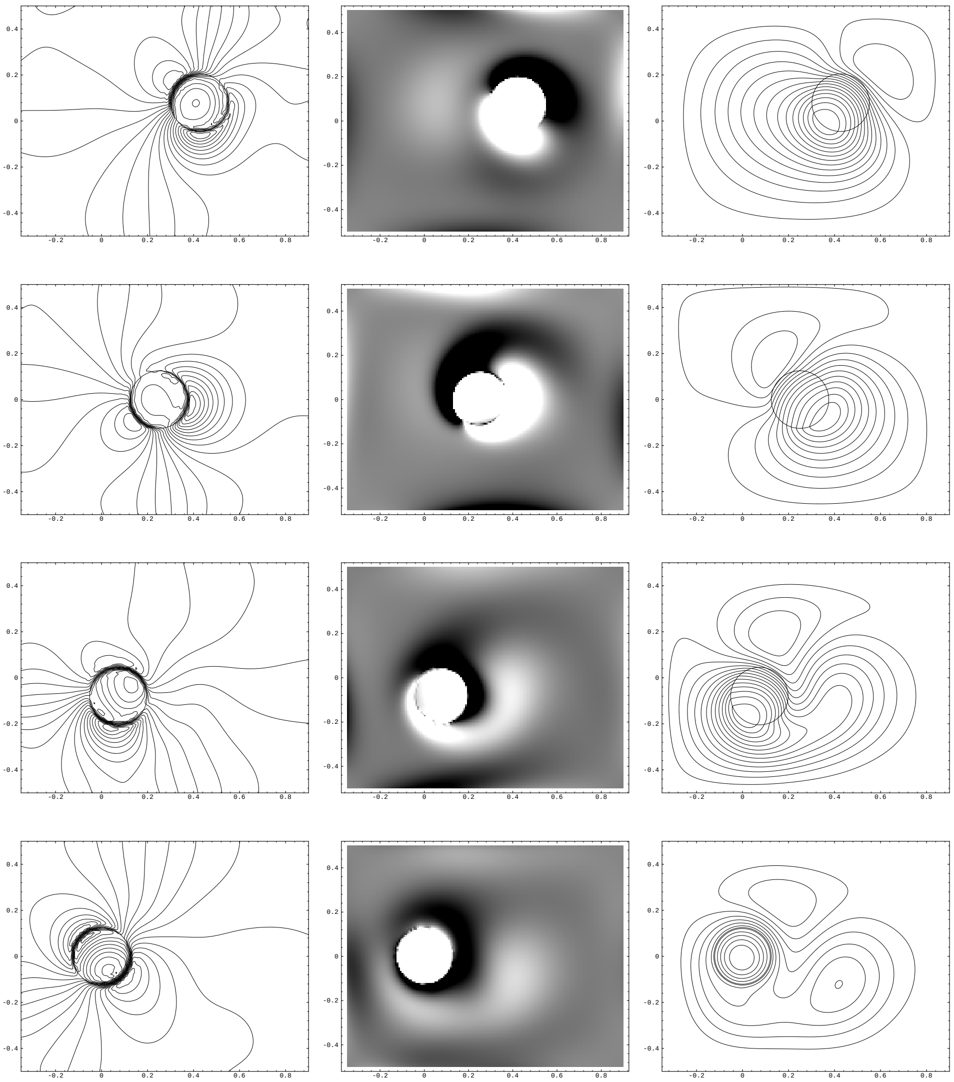

Figure 5 Isobar contours (at left), vorticity density (at middle) and streamlines (at right) at time $t = 6.5$, 7, 7.5, 8 during second half of one period of the disk motion. The disk is moving from the right to the left. The mesh size for velocity is $h = 1/128$ and the mesh size for pressure is $h = 1/64$.